Loss of CBP causes T cell lymphomagenesis in synergy with p27^{Kip1} insufficiency

Ningling Kang-Decker,[1] Caili Tong,[1] Fayçal Boussouar,[3] Darren J. Baker,[1] Wu Xu,[3] Alexey A. Leontovich,[2] William R. Taylor,[2] Paul K. Brindle,[3] and Jan M.A. van Deursen[1,*]

[1]Department of Pediatric and Adolescent Medicine and Department of Biochemistry and Molecular Biology
[2]Mayo Clinic Cancer Center, Mayo Clinic, 200 First Street SW, Rochester, Minnesota 55905
[3]Department of Biochemistry, St. Jude Children's Research Hospital, 332 North Lauderdale, Memphis, Tennessee 38105
*Correspondence: vandeursen.jan@mayo.edu

Summary

CBP can function as a tumor suppressor, but the mechanisms that govern oncogenesis in its absence are unknown. Here we show that CBP inactivation in mouse thymocytes leads to lymphoma. Although CBP has been implicated in the transactivation functions of p53, development of these tumors does not seem to involve loss of p53 activity. CBP-null tumors show reduced levels of p27^{Kip1} and increased levels of cyclin E and Skp2, two oncoproteins that can promote p27^{Kip1} proteolysis. Reduction of p27^{Kip1} by introduction of a p27^{Kip1}-null allele into CBP knockout mice accelerates lymphomagenesis and seems to obviate the requirement for Skp2 and cyclin E upregulation. These data suggest that CBP loss mediates lymphomagenesis in cooperation with a mechanism that reduces p27^{Kip1} abundance.

Introduction

CBP and p300 are highly related mammalian transcriptional coactivators that regulate gene transcription through various activities (Goodman and Smolik, 2000). Both coactivators are known to enhance gene transcription by linking sequence-specific transcription factors to the RNA polymerase II holoenzyme (Kee et al., 1996; Nakajima et al., 1997). They also promote gene transcription by forcing chromatin into conformations that are more accessible to DNA binding transcription factors through the acetylation of histones (Ogryzko et al., 1996). Besides histones, CBP and p300 also acetylate specific transcription factors. For instance, acetylation of p53 by CBP has been shown to enhance the DNA binding ability of p53 (Gu et al., 1997; Liu et al., 1999; Sakaguchi et al., 1998), and acetylation of CREB has been shown to stimulate CREB-mediated gene expression (Lu et al., 2003).

Mice lacking CBP or p300, or that are heterozygous for both CBP and p300, typically die around day 10.5 of embryogenesis with severe developmental retardation, reduced size, defects in heart development, and lack of neural tube closure (Oike et al., 1999; Yao et al., 1998). Although this confirms the notion that CBP and p300 are functionally conserved paralogs, specific differences in phenotype between the CBP- and p300-null embryos suggest that these coactivators also have nonredundant functions. For example, only CBP-null embryos exhibit defects in primitive hematopoiesis (Oike et al., 1999; Yao et al., 1998). CBP heterozygous mice, but not p300 heterozygous mice, show craniofacial and skeletal defects that are reminiscent of Rubinstein-Taybi syndrome (RTS) (Yao et al., 1998), a human disorder caused by monoallelic mutations in the CBP gene (Petrij et al., 1995). Furthermore, CBP heterozygous mice show reduced self-renewal capacity of hematopoietic stem cells, while p300 heterozygous mice do not (Rebel et al., 2002). Lastly, mice with point mutations in the p300 KIX domain that disrupt the binding surface for the transcription factors c-Myb and CREB show severe hematopoietic abnormalities including anemia, B cell deficiency, thymic hypoplasia, megakaryocytosis, and thrombocytosis (Kasper et al., 2002). By contrast, age-matched mice with identical mutations in the CBP KIX domain appear essentially normal.

Several lines of evidence suggest the involvement of CBP and p300 in tumor formation. CBP and p300 are at the breakpoints of several chromosomal translocations in human leukemias (reviewed in Blobel, 2000; Goodman and Smolik, 2000), and provide coactivator functions to translocation generated fusion proteins such as NUP98-HOXA9 and MOZ-TIF2 (Deguchi et al., 2003; Kasper et al., 1999). CBP and p300 have also been implicated in the actions of viral oncoproteins such as human T cell leukemia virus 1 (HTLV-1) Tax protein, adenovi-

SIGNIFICANCE

The coactivator CBP supplies adaptor molecule and protein acetyltransferase functions to a multitude of transcription factors and can contribute to the pathogenesis of human malignancies through oncogenic as well as tumor-suppressive functions. The mechanisms that govern cell transformation in the absence of CBP are unknown, largely because of the embryonic lethality of CBP-null mice. We found that conditional inactivation of CBP in thymocytes leads to lymphoma. Although the diverse and complex nature of CBP in transcriptional regulation suggests that its loss may promote tumorigenesis by deregulation of any variety of tumor suppressor and oncogenic pathways, this study indicates that CBP-mediated lymphomagenesis may involve a narrowly defined array of cooperative events that includes alterations that act to reduce p27^{Kip1} abundance.

rus E1A protein, simian virus (SV) 40 T antigen, and human papillomavirus (HPV) E6 (reviewed in Goodman and Smolik, 2000). Mutations of p300 have been found in several epithelial cancers, including breast and colon. In some of these tumors, loss of heterozygosity has been detected, suggesting that p300 may act as a tumor suppressor (Gayther et al., 2000; Muhua et al., 1998). Although no mutations have been reported in the CBP gene of such cancers (Ozdag et al., 2002), individuals with Rubinstein-Taybi syndrome have an increased tendency to develop tumors at an early age. CBP heterozygous mice develop a variety of hematopoietic defects that become apparent at about 3 months of age (Kung et al., 2000). When 18 such mice were aged, 7 developed hematological tumors (1 lymphatic leukemia, 1 myelogenous leukemia, 1 multiple myeloma, and 4 histiocytic sarcomas), with three tumors exhibiting loss at the remaining wild-type CBP gene locus. Hematological malignances also were found in chimeric mice derived by using $CBP^{-/-}$ or $p300^{-/-}$ embryonic stem cells. In this instance, one out of the 10 adult $CBP^{-/-}$ chimera mice developed T cell lymphoma, whereas four out of seven $p300^{-/-}$ chimeras developed histiocytic sarcoma (Rebel et al., 2002).

Although these studies indicate that CBP has the features of a tumor suppressor, the genetic changes that govern oncogenesis in its absence are unknown. Using a conditional knockout approach, we obtained viable mice with CBP disruption in a variety of tissues, including skin, thymus, salivary gland, spleen, mammary gland, and bone marrow. We found that these mice develop clonally derived T cell lymphomas with distinctive gene expression signatures. We show that reduced expression of $p27^{Kip1}$, which correlates with tumor aggressiveness and poor prognosis in many human cancers, plays a causal role in CBP-mediated lymphomagenesis, and we provide insight into the possible mechanism by which this reduction is established.

Results

Conditional inactivation of *CBP* in mice

To bypass the embryonic lethality caused by CBP deficiency, we generated mice with a CBP conditional knockout allele (CBP^{flox}) (Figure 1A). The generation of these mice is described in detail in the Supplemental Data at http://www.cancercell.org/cgi/content/full/5/2/177/DC1. Intercrosses of $CBP^{+/flox}$ mice yielded $CBP^{+/+}$, $CBP^{+/flox}$, and $CBP^{flox/flox}$ offspring at the Mendelian ratio (Figure 1B). $CBP^{flox/flox}$ mice were indistinguishable from their wild-type littermates and had a normal lifespan, indicating that the activity of the floxed CBP allele was similar to that of the wild-type allele.

To test whether CBP exerts tumor suppression activity, we crossed $CBP^{flox/flox}$ mice with MMTV-Cre transgenic mice that induce deletion of loxP-flanked alleles to mammary and salivary glands, skin, and certain hematopoietic cells (Wagner et al., 1997). MMTV-Cre|$CBP^{flox/flox}$ mice were born alive and showed no overt abnormalities. We verified Cre-mediated deletion of exon 9 in various tissues from 2-month-old MMTV-Cre|$CBP^{flox/flox}$ mice by Southern blot analysis (Figure 1C). As expected, extensive disruption of CBP occurred in mammary gland, salivary gland, skin, and hematopoietic cells in bone marrow, thymus, and spleen, while no detectable disruption occurred in skeletal muscle, testis, brain, lung, liver, kidney, and heart.

To verify that Cre-recombination created a null allele (CBP^{-}), we stained thymus, lymph node and bone marrow cells from 2-month-old $CBP^{flox/flox}$ and MMTV-Cre|$CBP^{flox/flox}$ mice with polyclonal antibodies against the amino or carboxy termini of CBP. Virtually all thymocytes from $CBP^{flox/flox}$ mice were positive for CBP (Figure 2A). In contrast, no CBP staining was seen in approximately 65% (SD = ± 19%, n = 3) of thymocytes from MMTV-Cre|$CBP^{flox/flox}$ mice (Figure 2A). Among affected thymocytes were $CD4^{-}CD8^{-}$ (DN), $CD4^{+}CD8^{+}$ (DP), $CD4^{-}CD8^{+}$, and $CD4^{+}CD8^{-}$ (SP) cells. Likewise, B220-positive B cells from $CBP^{flox/flox}$ mice typically stained positive for CBP, while only a subset of the corresponding cell types from MMTV-Cre|$CBP^{flox/flox}$ mice expressed CBP (Figure 2B). There was no detectable inactivation of CBP in bone marrow granulocytes (Figure 2C). Further immunohistochemical analysis showed that CBP protein was not expressed in the majority of mammary gland epithelial cells from MMTV-Cre|$CBP^{flox/flox}$ females (data not shown). Thus, CBP inactivation occurs in the expected tissues and cell types.

High incidence of fatal T cell lymphomas in MMTV-Cre|$CBP^{flox/flox}$ mice

We then generated a cohort of 70 MMTV-Cre|$CBP^{flox/flox}$ mice and monitored them for development of overt tumors or ill health. Fifty-nine percent of these mice developed fatal T cell lymphomas between 3 and 9 months of age (Figure 3A). Histological analysis of tumor sections typically showed a monotonous infiltrate of lymphoblasts with numerous mitotically active cells (Figures 3C and 3D). Extensive lymphoblast infiltration generally occurred in nonlymphoid and lymphoid organs including lung, liver, kidney, spleen, and lymph nodes (Figure 3E). Immunohistochemical and Western blot analysis of lymphoma tissue from six mice demonstrated a complete lack of CBP protein in each of the tumors (Figures 4A and 4B). By contrast, expression of p300 appeared normal (Figure 4A′). Twenty-nine MMTV-Cre|$CBP^{flox/flox}$ mice stayed healthy during the observation period of 10 months, as did the 40 $CBP^{flox/flox}$ and 15 MMTV-Cre|$CBP^{+/+}$ mice that served as control groups (Figure 3A). Analysis of the thymuses of two long-term surviving MMTV-Cre|$CBP^{flox/flox}$ mice for Cre-recombination showed a lack of CBP in 96% and 51% of thymocytes, respectively, confirming that their CBP disruption frequency is similar to that of the mice that develop tumors.

We further characterized tumors from MMTV-Cre|$CBP^{flox/flox}$ mice by immunophenotyping. Tumor samples were primarily $CD4^{+}$, $CD8^{+}$, and $CD3^{+}$, matching the cell surface marker profile of late cortical thymocytes (see Figure 4D and Supplemental Table S1 at http://www.cancercell.org/cgi/content/full/5/2/177/DC1). Lymphoblasts from these tumors generally expressed remarkably high levels of the IL-2 receptor α chain. One of 15 tumors analyzed exhibited a $CD4^{-}$, $CD8^{+}$, and $CD3^{+}$ mature T cell profile (Supplemental Table S1). All tumors were negative for the B cell marker B220. Next, DNA was isolated from 9 tumors and analyzed for T cell receptor (TCR) β chain gene rearrangements by Southern blot hybridization to a TCR Cβ2 probe. Each of the tumors showed one or two discrete bands indicative of the clonal origin of the lymphomas (Figure 4C).

Altered thymocyte development in MMTV-Cre|$CBP^{flox/flox}$ mice

To define possible effects of CBP disruption on thymocyte development, we collected thymuses from preleukemic 8-week-old MMTV-Cre|$CBP^{flox/flox}$ mice and analyzed their thymocytes

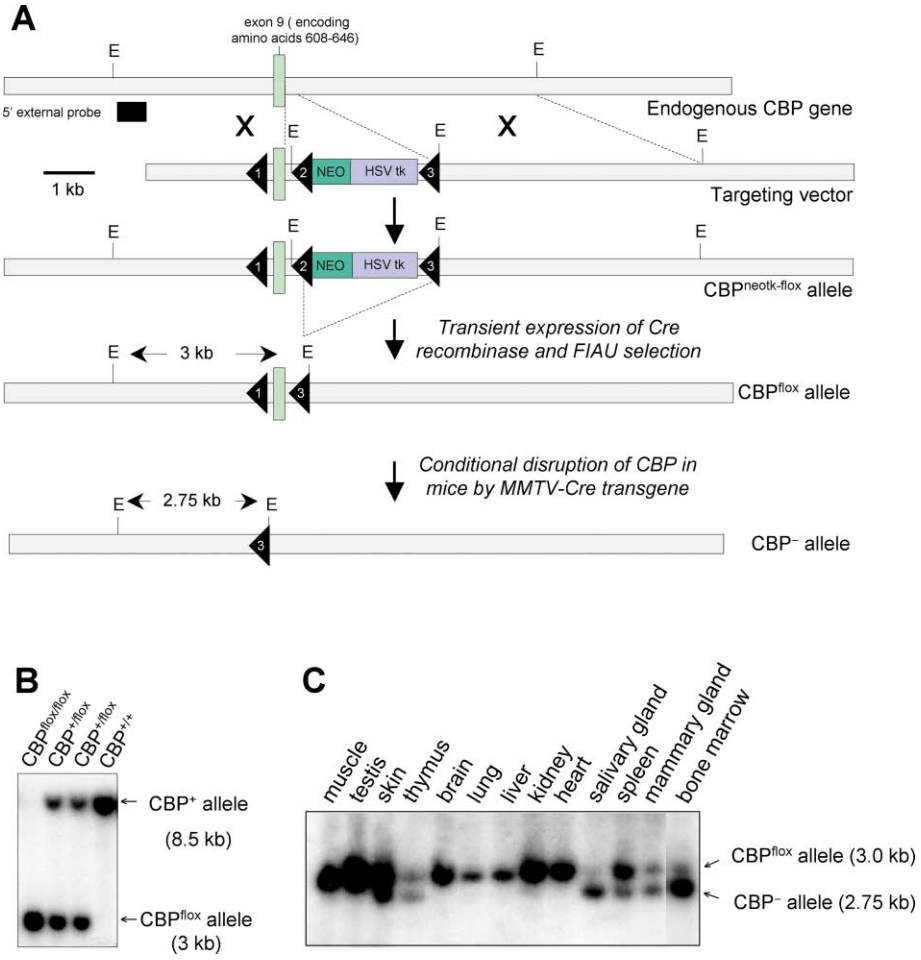

Figure 1. Generation of CBP conditional knockout mice

A: Schematic of the endogenous CBP locus, the targeting vector, and various mutant CBP alleles. LoxP recombination sites used to generate the CBP^{flox} allele are shown as triangles. EcoRI restriction sites used for Southern blot identification of mutant CBP alleles are indicated, as is the external hybridization probe. Abbreviations: NEO, neomycin resistance gene; HSV tk, herpes simplex virus thymidine kinase gene.

B: Southern blot of EcoRI-digested tail DNA from $CBP^{+/+}$, $CBP^{+/flox}$ $CBP^{flox/flox}$ mice. Sizes of the bands representing the CBP^{+} and CBP^{flox} alleles are indicated. The genotypes are displayed above the lanes.

C: Southern blot analysis of EcoRI-digested DNA from various tissues of an 8-week-old MMTV-Cre|$CBP^{flox/flox}$ female mouse (the testis sample was from a male mouse of the same genotype). The sizes of the bands representing the CBP^{flox} and CBP^{-} alleles are indicated.

by flow cytometry. There were on average 2×10^8 thymocytes per MMTV-Cre|$CBP^{flox/flox}$ mouse (SD = $\pm$ 0.3×10^8, n = 4 mice) versus 1.7×10^8 thymocytes per $CBP^{flox/flox}$ mouse (SD = $\pm$ 0.6×10^8, n = 4 mice). CD4 and CD8 staining of thymocytes confirmed that all subpopulations of thymocytes were present in MMTV-Cre|$CBP^{flox/flox}$ mice (Figure 4D). The percentages of DN and CD4-SP thymocytes were comparable in MMTV-Cre|$CBP^{flox/flox}$ and $CBP^{flox/flox}$ mice. However, the percentages of the CD8-SP thymocytes were significantly increased in MMTV-Cre|$CBP^{flox/flox}$ mice compared to $CBP^{flox/flox}$ mice (21% $\pm$ 9% [n = 8] versus 2% $\pm$ 0.5% [n = 5]). Concomitantly, the percentages of DP thymocytes were significantly reduced in MMTV-Cre|$CBP^{flox/flox}$ mice compared to $CBP^{flox/flox}$ mice (61% $\pm$ 9% [n = 8] versus 82% $\pm$ 2% [n = 5]). These data suggest that the cell fate decision process in DP thymocytes may require specific CBP functions that cannot be substituted by p300, or may depend on a certain amount of total CBP/p300 protein.

CBP-null tumors retain p53 responses to DNA damage

Numerous studies have highlighted a role of CBP and p300 in the p53 signaling pathway (reviewed by Goodman and Smolik, 2000; Grossman, 2001). CBP and p300 physically interact with p53 and modulate p53 transcriptional activity (Avantaggiati et al., 1997; Gu et al., 1997; Lill et al., 1997). In response to DNA damage or other stress-inducing agents, CBP and p300 acetylate p53 at specific sites (Ito et al., 2001; Sakaguchi et al., 1998). The acetylation seems to play a role in stabilization of p53 through inhibition of its ubiquitination by Mdm2 (Ito et al., 2001; Li et al., 2002). Because most p53-null mice, like MMTV-Cre|$CBP^{flox/flox}$ mice, develop T cell lymphoma, we hypothesized that loss of CBP may contribute to tumorigenesis through inactivation of p53 tumor suppressor functions (Giordano and Avantaggiati, 1999). To test this idea, we performed two experiments involving ionizing radiation to activate p53. First, we exposed 20 MMTV-Cre|$CBP^{flox/flox}$ and 9 $CBP^{flox/flox}$ mice to a 1 Gray (Gy) dose of whole body γ irradiation at 14 and 21 days of age and monitored them for the development of tumors. We verified by immunolabeling that a substantial proportion of thymocytes lacked CBP at the age of irradiation (55% $\pm$ 7, n = 3). Previous work has shown that irradiation of pre-weanling $p53^{-/-}$ mice with 1 Gy of ionizing irradiation decreases the tumor latency from a median of 21 weeks to 14–15 weeks of age (Kemp et al., 1994). Thus, if loss of CBP results in functional inactivation of p53's tumor suppression activity, then one would expect to find MMTV-Cre|$CBP^{flox/flox}$ mice susceptible to radiation-induced T cell lymphomagenesis. As shown in Figure 5A, ionizing irradiation did not decrease the latency for T cell tumor development in MMTV-Cre|$CBP^{flox/flox}$ mice, suggesting that the p53 response to γ irradiation-induced DNA damage is intact in the absence of CBP. In the second experiment, we measured the p53 response

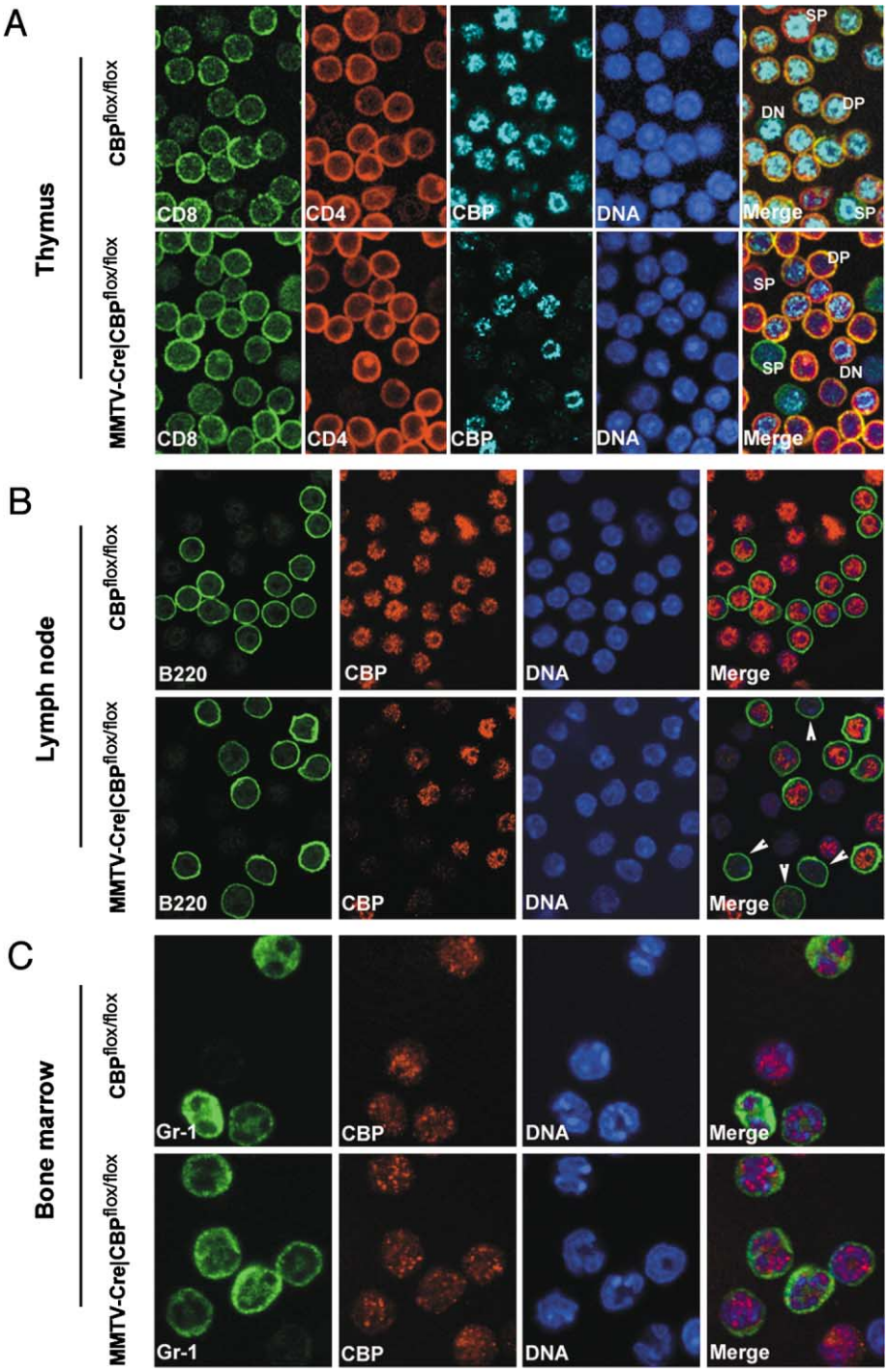

Figure 2. Cre recombinase activity in hematopoietic cells of MMTV-Cre|CBP$^{flox/flox}$ mice

A–C: Representative confocal images of cells from various hematopoietic tissues of 8-week-old CBP$^{flox/flox}$ and (preleukemic) MMTVCre|CBP$^{flox/flox}$ mice stained for various proteins. **A:** Thymocytes triple-labeled with CD8, CD4, and CBP antibodies. Note that the majority of MMTVCre|CBP$^{flox/flox}$ thymocytes are negative for CBP and that DN, DP, and both types of SP thymocytes were among the negative cells. **B:** Lymph node cells double-labeled with B220 and CBP. Arrowheads mark B220-positive B cells that lack CBP. **C:** Bone marrow cells double-stained for myelocyte marker Gr-1 and CBP. Note that no significant Cre-mediated inactivation occurs in myelocytes.

following irradiation of CBP-null tumors. Lymphomas were harvested from MMTV-Cre|CBP$^{flox/flox}$ mice (n = 7) and cell suspensions from these tumors were treated with 5 Gy of ionizing irradiation. For comparison, thymocytes from CBP$^{flox/flox}$ mice were treated similarly. p53 protein levels, which were low before irradiation, as expected, showed a strong increase at 4 hr after treatment for both tumor cells lacking CBP and control thymocytes (Figure 5B). By 8 hr after irradiation, p53 protein levels were decreased in both tumor and control cells. These results indicate that CBP is dispensable for p53 induction in response to radiation-induced DNA damage. After DNA damage, p53 normally activates a number of transcriptional targets, including the cyclin-dependent kinase inhibitor p21$^{Waf/Cip1}$. Indeed, the level of p21$^{Waf/Cip1}$ increased in both normal and tumor cells, with tumor cells showing an even more robust increase than control cells (Figure 5B). Irradiated preleukemic MMTV-Cre|CBP$^{flox/flox}$ thymocytes showed levels of p21$^{Waf/Cip1}$ induction that were similar to those of control thymocytes. Moreover, when CBP-null tumor cells were analyzed for p53-dependent radiation-induced apoptosis by standard methods (Lowe et al., 1993), similar death

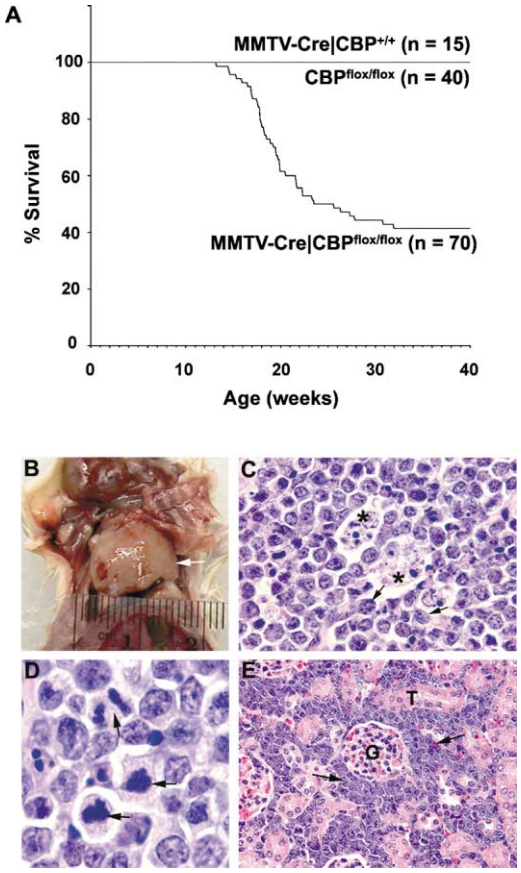

Figure 3. MMTV-Cre|CBP$^{flox/flox}$ mice develop lethal T cell lymphomas

A: Kaplan-Meier tumor-free survival curve of MMTV-Cre|CBP$^{flox/flox}$, CBP$^{flox/flox}$, and MMTV-Cre|CBP$^{+/+}$ mice. The median tumor-free survival period of MMTV-Cre|CBP$^{flox/flox}$ mice was 24 weeks.
B: Gross morphology of a representative T cell lymphoma (arrow).
C–E: Histopathology of tumors from moribund MMTV-Cre|CBP$^{flox/flox}$ mice (hematoxylin and eosin-stained paraffin sections). **C:** Large macrophages with nuclear debris of lymphocytes in their cytoplasm (asterisks) embedded in uniform populations of highly mitotic thymic lymphoblasts (arrows). **D:** Detail of mitotic lymphoblasts (arrows). **E:** Lymphoma cells (arrows) infiltrated in kidney tissue (G marks a glomerulus and a renal tubule).

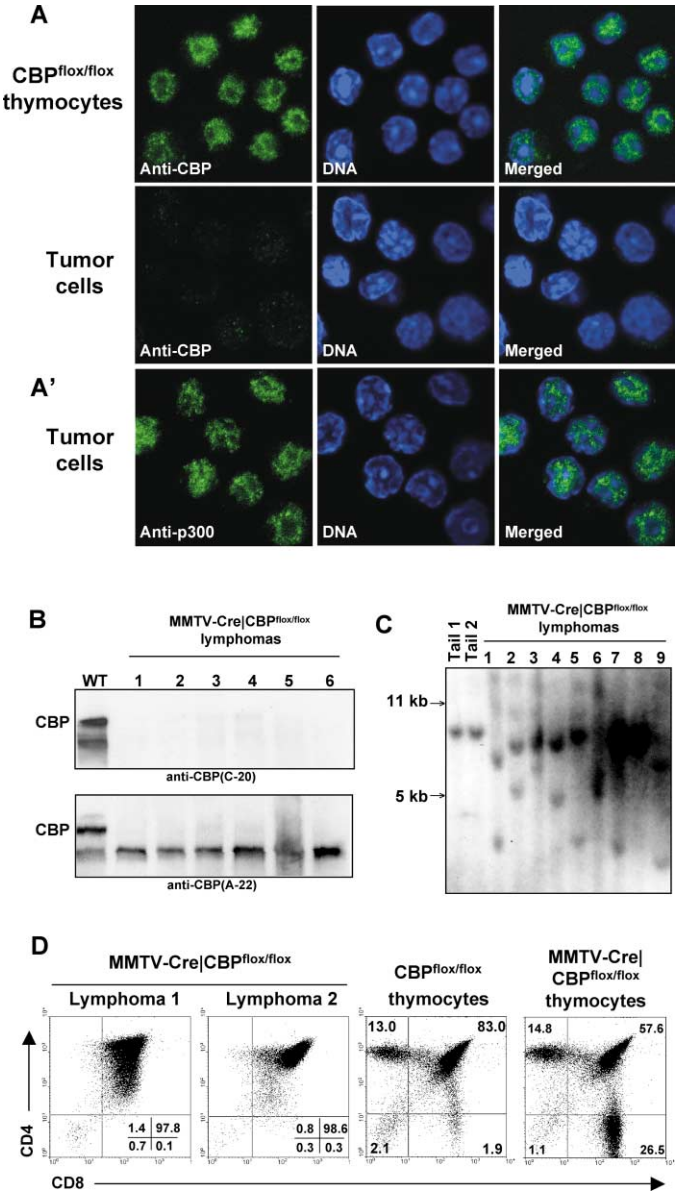

Figure 4. Lymphomas consist of mono- or oligoclonal populations of DP thymocytes that lack CBP

A: Representative confocal images of cells from a wild-type thymus and a T cell lymphoma stained with CBP antibodies and Hoechst.
A': Confocal images of cells from a T cell lymphoma stained with p300 antibodies and Hoechst, demonstrating that CBP disruption does not interfere with p300 expression.
B: Analysis of lymphomas from distinct MMTV-Cre|CBP$^{flox/flox}$ mice for CBP protein levels by Western blotting. 100 μg of total protein extract from each tumor was used in the analysis. For probes, we used a rabbit antibody against CBP(C-20) or anti-CBP(A-22).
C: SacI-digested genomic DNAs extracted from T cell lymphomas analyzed by Southern blot hybridization to the TCR Cβ2 probe. All MMTV-Cre|CBP$^{flox/flox}$-derived lymphomas tested show one or two discrete rearranged fragments, reflecting clonal expansion.
D: CD4/CD8 FACS profiles of thymocytes from 8-week-old CBP$^{flox/flox}$ and MMTV-Cre|CBP$^{flox/flox}$ mice, and cells from tumors of two moribund MMTV-Cre|CBP$^{flox/flox}$ mice.

rates were observed in normal thymocytes and cells from CBP-null tumors (data not shown; n = 2 independent tumors).

Next, we employed DNA microarray technology to generate expression profiles of two p53-null and three CBP-null tumors (all five tumors were DP). Hierarchical clustering analysis of the resulting gene expression data grouped the p53-null and CBP-null tumors in two clearly distinguishable branches, suggesting that their transformation pathways were distinct (Figure 5D). At least 60 genes were differentially expressed more than 2-fold between the two tumor types ($p < 0.01$ by two-tailed t test). These results strongly suggest that the tumorigenic mechanisms operating in the two lymphoma types were dissimilar and reinforced the notion that loss of CBP promotes tumorigenesis through a mechanism that does not involve p53 inactivation.

Disruption of p53 accelerates tumorigenesis in CBP conditional knockout mice

Although CBP does not seem to play a critical role in the p53-dependent DNA damage pathway, other pathways that regulate

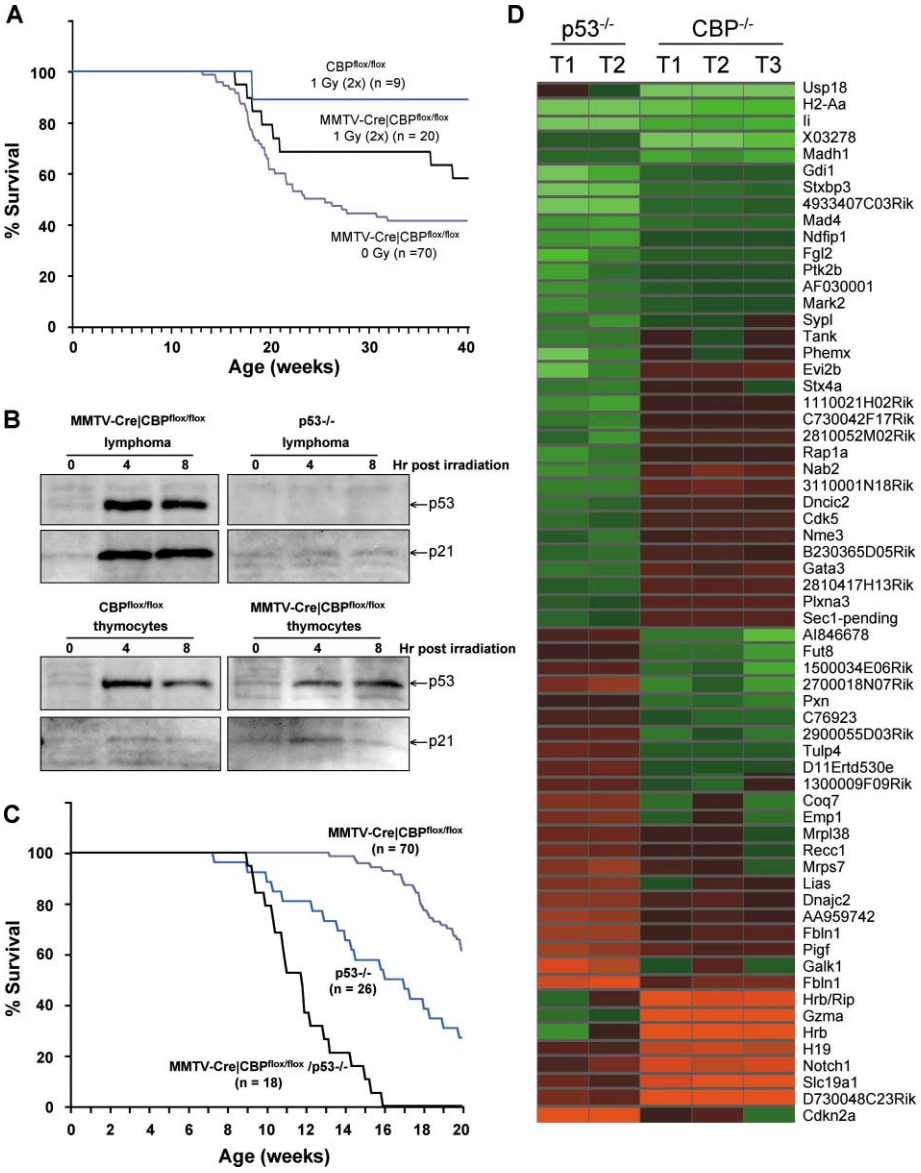

Figure 5. Loss of CBP does not abolish p53 tumor suppression activity

A: Survival curves of irradiated MMTV-Cre|CBP$^{flox/flox}$, irradiated CBP$^{flox/flox}$, and nonirradiated MMTV-Cre|CBP$^{flox/flox}$ mice.

B: Analysis of p53 and p21$^{Waf1/Cip1}$ protein levels in T cell tumor cells from MMTV-Cre|CBP$^{flox/flox}$ and p53$^{-/-}$ mice and in thymocytes from 8-week-old CBP$^{flox/flox}$ and MMTV-Cre|CBP$^{flox/flox}$ mice before and after 5 Gy of ionizing irradiation. Results shown are representative for 3 experiments in which tumor cells from 7 moribund MMTV-Cre|CBP$^{flox/flox}$ mice were evaluated.

C: Survival curves of MMTV-Cre|CBP$^{flox/flox}$, MMTV-Cre|CBP$^{flox/flox}$;p53$^{-/-}$, and p53$^{-/-}$ mice. All MMTV-Cre|CBP$^{flox/flox}$;p53$^{-/-}$ mice died of T cell lymphoma before the age of 16 weeks (lower line). By contrast, 93% of MMTVCre|CBP$^{flox/flox}$ mice (upper line) and 57% of p53$^{-/-}$ mice (middle line) were alive at 16 weeks.

D: Hierarchical heat map of genes differentially expressed an average more than 2-fold between CBP-null (CBP) and p53-null (p53) T cell lymphomas. Only probe sets that were identified as differentially expressed between the two tumor types by two-tailed t test were included ($p < 0.01$). Data is presented as a signed ratio between the expression signal for individual tumors and the mean signal for two normal CBP$^{flox/flox}$ thymuses (green = −6-fold, red = +6-fold).

p53 activity could still be disrupted. To test for this possibility, we crossed CBP conditional knockout mice onto a p53-null background and observed them for tumor formation. If combined loss of CBP and p53 tumor suppression pathways would significantly decrease tumor latency, then this would strengthen the idea that p53 tumor suppression activity remains intact in the absence of CBP. We produced cohorts of MMTV-Cre|CBP$^{flox/flox}$;p53$^{-/-}$ and CBP$^{flox/flox}$;p53$^{-/-}$ mice and observed them daily for development of tumors or ill health. The CBP$^{flox/flox}$;p53$^{-/-}$ mice developed T cell lymphomas with a median tumor-free survival period of 16 weeks (Figure 5C). By contrast, MMTV-Cre|CBP$^{flox/flox}$;p53$^{-/-}$ developed T cell lymphomas with a much shorter median tumor-free survival period of 12 weeks, with none of the animals surviving beyond 16 weeks. PCR genotyping revealed that all tumors from MMTV-Cre|CBP$^{flox/flox}$;p53$^{-/-}$ mice were homozygous for the Cre-recombined CBP-null allele (data not shown).

DNA microarray analysis of preleukemic thymocytes

To identify gene deregulations that might explain why CBP-null thymocytes are predisposed to tumor formation, we generated expression profiles of preleukemic DP thymocytes by DNA microarray analysis. DP thymocytes were selected for analysis because >90% of the CBP-null tumors originated from this cell type. We collected thymuses of two 8-week-old MMTV-Cre|CBP$^{flox/flox}$ and two CBP$^{flox/flox}$ mice, purified DP thymocytes by FACS (40%–65% of the sorted cells from the MMTV-Cre|CBP$^{flox/flox}$ mice lacked CBP), and isolated RNA from each of the four samples for hybridization to AFFY_MOE430A chips (containing 14,092 genes). By cluster analysis, we identified a set of eight genes whose levels were reproducibly changed ≥2 fold by the loss of CBP (see Supplemental Table S2 at http://www.cancer cell.org/cgi/content/full/5/2/177/DC1), but it provided no clues about the events that might initiate lymphomagenesis in CBP-deficient thymocytes. This result indicates that loss of CBP may act to increase the susceptibility of tumor

development by subtle deregulation of a large number of targets rather than by severely impairing the activities of a small number of cancer-causing genes. Another possibility is that CBP loss may only exert its tumor-promoting effect after a CBP-null cell has undergone a mutation in a particular cancer-critical gene.

CBP acts synergistically with p27^{Kip1} in tumor suppression

The time to onset of tumor formation and the clonal derivation of the tumors indicated that cooperative events are implicated in the development of lymphoma in CBP conditional knockout mice. Genetic events that disrupt key regulators of G_1 progression are found in most human cancers, including lymphomas (Erlanson et al., 1998). This prompted us to analyze tumor samples from MMTV-Cre|CBP$^{flox/flox}$ mice for altered expression of such regulators by Western blot analysis. We found that cyclin D1, cyclin A, CDK2, and CDK4 were all expressed at similar levels in tumors and normal thymuses (data not shown). However, with 100% penetrance, p27^{Kip1} was expressed at substantially lower levels in tumor cells (Figure 6A, lanes 3–8; n = 15 mice) than in thymocytes from CBP$^{flox/flox}$ mice (lanes 1 and 2; n = 4 mice), thymocytes from preleukemic MMTV-Cre|CBP$^{flox/flox}$ mice (Figure 6B and C; n = 4 mice), and thymocytes from CBP$^{flox/flox}$ mice that were stimulated with the mitogen PHA (Figure 6B, lanes 8–10; n = 3 mice, see also Supplemental Experimental Procedures and Supplemental Figure S1 at http://www.cancercell.org/cgi/content/full/5/2/177/DC1). In addition, cyclin E levels were always much higher in tumor cells (Figure 6A, lanes 3–8) than in the various control thymocytes (Figure 6A and 6B). Importantly, low p27^{Kip1} and high cyclin E levels have been found in a variety of human cancers, either alone or in combination, and correlate with reduced long-term survival (Catzavelos et al., 1997; Loda et al., 1997; Porter et al., 1997).

The fact that a substantial proportion of CD4$^+$CD8$^+$ lymphomas induced by Moloney murine leukemia virus (MuLV) retain high levels of p27^{Kip1} protein (Martins and Berns, 2002) suggests that p27^{Kip1} is not simply downregulated due to increased proliferation of tumor cells compared to normal thymocytes. To establish whether the reduced expression of p27^{Kip1} in CBP-null tumors might be a deregulation that cooperates with CBP loss in T cell lymphomagenesis, CBP conditional knockout mice were interbred with p27^{Kip1} knockout mice to generate MMTV-Cre|CBP$^{flox/flox}$;p27$^{Kip1+/-}$ mice, which were monitored for tumor formation (disruption of a single p27^{Kip1} allele is known to cause decreased p27^{Kip1} protein expression [Fero et al., 1998]). MMTV-Cre|CBP$^{flox/flox}$;p27$^{Kip1+/-}$ mice developed T cell lymphomas with a median tumor-free survival period of 12–13 weeks (Figure 6D; $p < 0.0001$ by the logrank test). For MMTV-Cre|CBP$^{flox/flox}$ mice on a similar genetic background, the median tumor-free survival period was 24 weeks. Consistent with previously reported studies (Fero et al., 1996, 1998), a cohort of 15 p27$^{Kip1+/-}$ control mice showed no T cell lymphoma development (data not shown). Western blots showed that tumor lysates from MMTV-Cre|CBP$^{flox/flox}$;p27$^{Kip1+/-}$ mice contained p27^{Kip1} protein, indicating that there was no loss of the wild-type p27^{Kip1} allele during tumorigenesis (data not shown). Taken together, the above data indicate a causal link between p27^{Kip1} insufficiency and tumor progression in CBP conditional knockout mice.

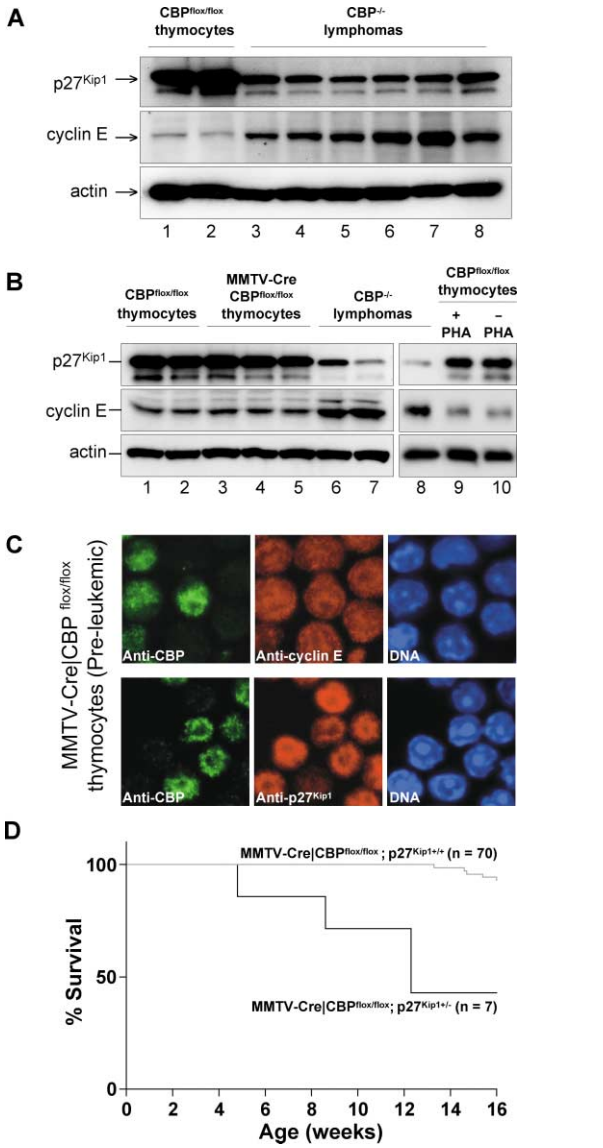

Figure 6. Loss of CBP synergizes with reduced expression of p27^{Kip1} in T cell lymphomagenesis

A and B: Western blot of p27^{Kip1} and cyclin E protein levels in lymphomas from moribund MMTV-Cre|CBP$^{flox/flox}$ mice, thymocytes from 8-week-old CBP$^{flox/flox}$ and (healthy) MMTV-Cre|CBP$^{flox/flox}$ mice, and thymocytes from 10-week-old CBP$^{flox/flox}$ mice that were cultured for 68 hr in the presence (+) or absence (−) of the mitogen PHA (20 μg/ml). Proliferation induction by PHA was verified by ^{3}H thymidine incorporation (see Supplementary Figure S1 at http://www.cancercell.org/cgi/content/full/5/2/177/DC1). 30 μg of total protein extract was loaded per lane.

C: Representative confocal images of thymocytes from an 8-week-old healthy MMTVCre|CBP$^{flox/flox}$ mouse double-labeled for p27^{Kip1} and CBP, or cyclin E and CBP. Note that p27^{Kip1} and cyclin E protein levels are similar in CBP-positive and negative cells prior to tumor formation.

D: Survival curves of MMTV-Cre|CBP$^{flox/flox}$ and MMTV-Cre|CBP$^{flox/flox}$;p27$^{Kip1+/-}$ mice. The median tumor free-survival period of MMTV-Cre|CBP$^{flox/flox}$;p27$^{Kip1+/-}$ mice was significantly decreased compared to MMTV-Cre|CBP$^{flox/flox}$ mice on a similar genetic background ($p < 0.0001$ by the logrank test).

Abnormal gene transcription and protein degradation downregulate p27^{Kip1} in CBP-null tumors

We investigated the mechanism of p27^{Kip1} downregulation during CBP-mediated lymphomagenesis, and first focused on Skp2. This F box protein normally accumulates in G_1 phase and targets p27^{Kip1} molecules that have been phosphorylated by cyclin E/Cdk2 for ubiquitin-mediated degradation at the G_1/S transition (Carrano et al., 1999). High levels of Skp2 are known to enhance p27^{Kip1} degradation (Blain et al., 2003; Bloom and Pagano, 2003), which prompted us to test for the possibility that Skp2 overexpression might be involved in the downregulation of p27^{Kip1} during CBP-mediated lymphomagenesis. As shown in Figure 7A, Skp2 protein levels were always higher in tumors from MMTV-Cre|CBP$^{flox/flox}$ mice (lanes 3–8; n = 9 mice) than in thymocytes from CBP$^{flox/flox}$ mice (lanes 1 and 2; n = 4 mice) or healthy 8-week-old MMTV-Cre|CBP$^{flox/flox}$ mice (data not shown). We reasoned that if this increase participates in CBP-mediated lymphomagenesis through downregulation of p27^{Kip1}, one would not expect to find it in tumors from MMTV-Cre|CBP$^{flox/flox}$; p27$^{Kip1+/-}$ mice. Indeed, high Skp2 levels were not seen in the tumors that we collected from four MMTV-Cre|CBP$^{flox/flox}$; p27$^{Kip1+/-}$ mice (Figure 7B, lanes 6–9). In addition, increased expression of cyclin E, which characterizes MMTV-Cre|CBP$^{flox/flox}$ tumors (Figure 6A) and which might act to enhance p27^{Kip1} phosphorylation and subsequent Skp2-mediated degradation (Blain et al., 2003), was not consistently seen in tumors from MMTV-Cre|CBP$^{flox/flox}$;p27$^{Kip1+/-}$mice (Figure 7B). The data suggest that the increases in Skp2 and cyclin E may act coordinately to induce unscheduled S phase entry through p27^{Kip1} downregulation.

To confirm that the mechanism of p27^{Kip1} reduction in CBP-null tumors involves proteosome-dependent protein degradation, we cultured MMTV-Cre|CBP$^{flox/flox}$ tumor cells for 6 hr in the presence or absence of the proteosome inhibitor MG132 (25 μM) and then measured p27^{Kip1} levels by Western blot analysis. As shown in Figure 7C (lanes 3–6), MG132-treated tumor cells had considerably higher p27^{Kip1} levels compared to their nontreated counterparts. As expected, normal thymocytes, which have low p27^{Kip1}degradation activity (Latres et al., 2001), showed similar p27^{Kip1} levels in the presence or absence of MG132 (lanes 1 and 2).

We next tested the possibility that reduced gene transcription contributed to p27^{Kip1} downregulation in CBP-null tumors by quantitative (Q)RT-PCR analysis. p27^{Kip1} mRNA levels were on average about 2-fold lower in tumor cells than in thymocytes from 8-week-old CBP$^{flox/flox}$ or MMTV-Cre|CBP$^{flox/flox}$ mice (Figure 7D). Together, our data suggest that downregulation of p27^{Kip1} levels in CBP-null tumors is established by decreased p27^{Kip1} gene transcription (and/or mRNA stability) and increased proteosome-dependent degradation of p27^{Kip1} protein.

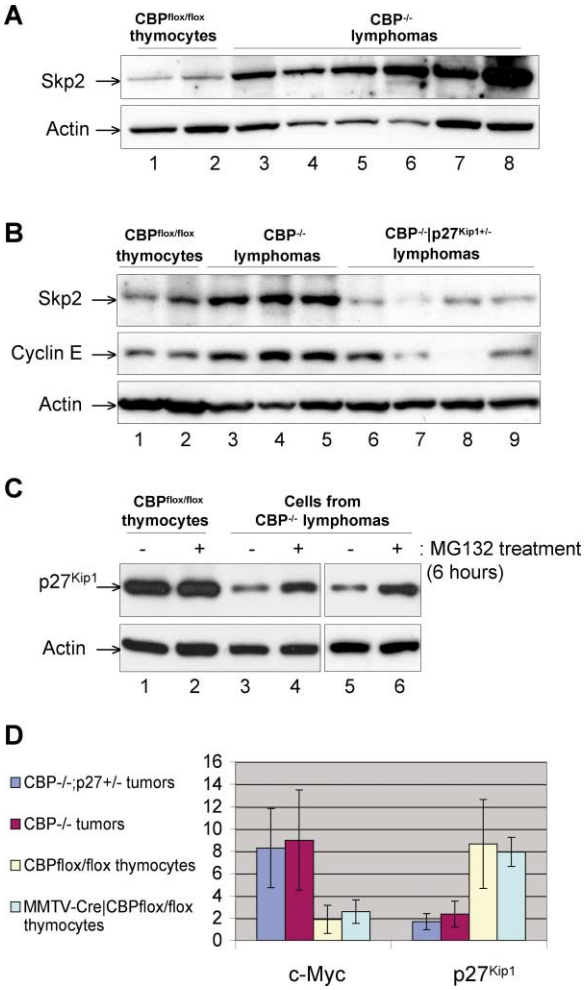

Figure 7. Negative regulators of p27^{Kip1} are expressed at increased levels in CBP-null tumors

A: Expression of Skp2 in thymocytes from two 8-week-old CBP$^{flox/flox}$ mice (lanes 1 and 2), and tumors from six individual MMTV-Cre|CBP$^{flox/flox}$ mice. Blots were respectively probed with Skp2 (SKP2-2B12, and actin antibody.

B: Levels of Skp2 and cyclin E in lymphomas from MMTV-Cre|CBP$^{flox/flox}$ and MMTV-Cre|CBP$^{flox/flox}$;p27$^{Kip1+/-}$ mice (the tumor in lane 8 showed cyclin E signal upon extended exposure of the blot).

C: Measurements of proteosome-dependent p27^{Kip1} degradation in tumor cells from two MMTV-Cre|CBP$^{flox/flox}$ mice and thymocytes from a CBP$^{flox/flox}$ control mouse using the proteosome inhibitor MG132.

D: Analysis of p27^{Kip1} and c-Myc gene expression levels QRT-PCR in thymocytes from 8-week-old CBP$^{flox/flox}$ (n = 2) and (healthy) MMTV-Cre|CBP$^{flox/flox}$ mice (n = 2) and tumor cells from MMTV-Cre|CBP$^{flox/flox}$ mice (n = 3) and MMTV-Cre|CBP$^{flox/flox}$;p27$^{Kip1+/-}$ mice (n = 4).

Protooncogenes Notch1, Bmi-1, and Myc are upregulated in CBP-null tumors

By comparing the transcriptional profiles of three CBP-null tumors to those of two control thymocytes, we identified 64 genes whose expression was changed more than 2-fold: 34 genes were decreased in activity, and 30 genes were more actively transcribed in tumor cells (Figure 8A). The latter group contained the transcription factors Notch1, Bmi-1, and Myc, all of which can cause T cell lymphomas in mice when ectopically expressed (Alkema et al., 1997; Fowlkes and Robey, 2002; Haupt et al., 1993; Martins and Berns, 2002). Validation experiments confirmed that Notch1 protein levels were substantially increased in 5 out of 6 tumors analyzed (Figure 8A, lanes 3–8; n = 6 independent mice). Several target genes that are regulated by Notch1, such as Adam9, Dtx1, and Hes-1, were expressed at considerably higher levels in tumors from CBP conditional knockout mice than in thymocytes from CBP$^{flox/flox}$ mice or healthy 8-week-old MMTV-Cre|CBP$^{flox/flox}$ mice (see Figure 8B). This result further confirmed that Notch1 activity increased during CBP-mediated tumorigenesis. In addition, Western blot experiments confirmed that Bmi-1 protein levels were substantially

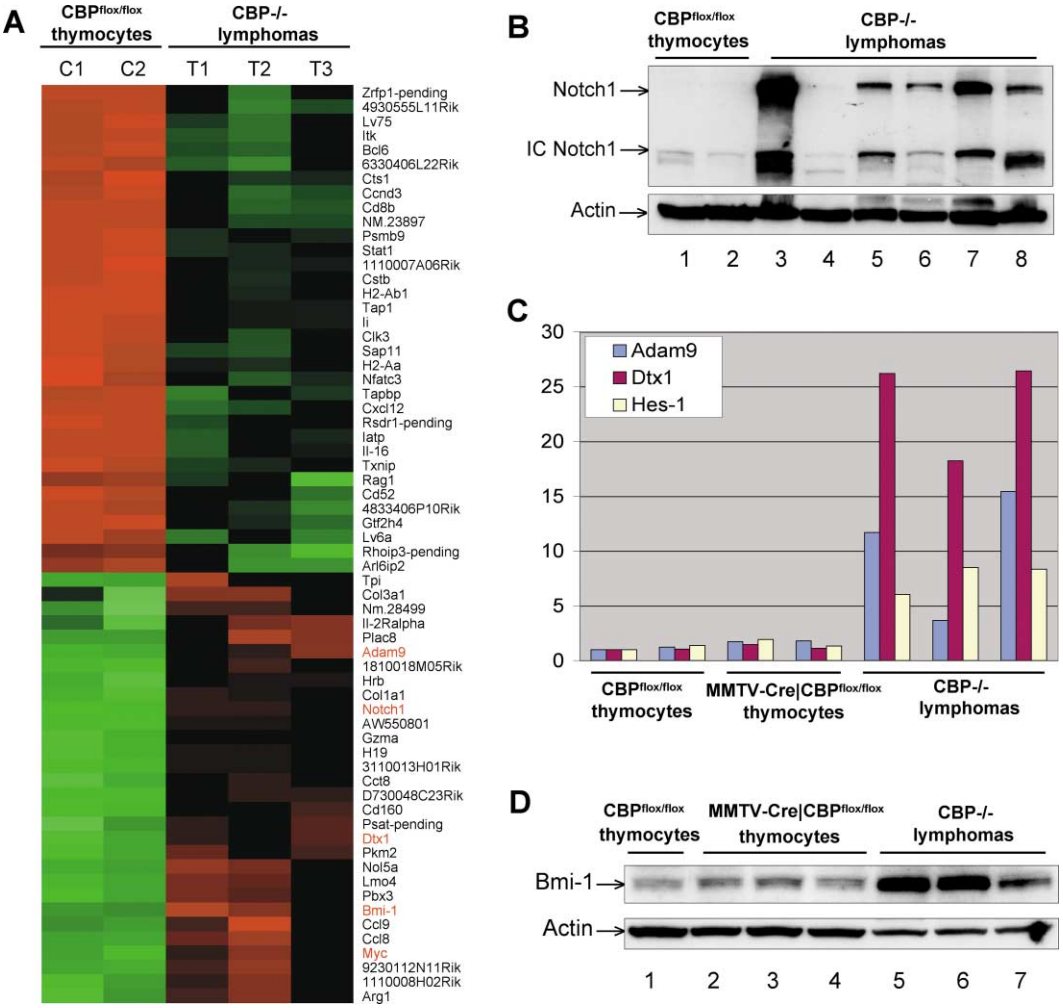

Figure 8. Expression signature of CBP-null tumors

A: Expression profiles of genes that were ≥2-fold changed in CBP-null tumors (n = 3) versus control ($CBP^{flox/flox}$) thymuses (n = 2). Data is presented as base 2 logarithm of signal values (green = signal value of 49, red = signal value of 54,000). Genes typed in red font were confirmed by QRT-PCR or Western blotting. We note that Skp2 probes were not on the U74 GeneChip, whereas $p27^{Kip1}$ probesets were scored absent by the Affymetrix software.
B: Confirmation of increased Notch1 expression in CBP-null tumors by Western blotting. Notch1-mN1A antibody, which detects both the full-length protein (Notch1) and the active intracellular domain of Notch1 (IC Notch1), was used as probe.
C: Confirmation of Notch1-target genes by QRT-PCR.
D: Confirmation of Bmi-1 overexpression in CBP-null tumors by Western blotting.

higher in 8 out of 9 lymphomas tested (lanes 5–7) compared to thymocytes from $CBP^{flox/flox}$ mice (lane 1; n = 3 thymuses) or healthy 8-week-old MMTV-Cre|$CBP^{flox/flox}$ mice (lanes 2–4; n = 3 thymuses). Although Bmi-1 has been shown to downregulate $p16^{Ink4a}$ gene transcription (Jacobs et al., 1999), we found no evidence for reduced expression of p16 and $p19^{Arf}$ in CBP-null tumors by expression profiling, QRT-PCR, or Western blot analysis (data not shown). QRT-PCR analysis for Myc showed that the expression of this protooncogene was on average 2- to 3-fold higher in tumors from MMTV-Cre|$CBP^{flox/flox}$ mice than in thymocytes from $CBP^{flox/flox}$ or healthy MMTV-Cre|$CBP^{flox/flox}$ mice (Figure 7D). Taken together, these results demonstrate that the protooncogenes Notch1, Bmi-1, and Myc are overexpressed in most CBP-null tumors, and suggest that their deregulation might play a role in CBP-mediated lymphomagenesis.

Discussion

By the use of CBP conditional knockout mice, we show that inactivation of CBP in the thymus leads to formation of lethal T cell lymphomas between 3 and 9 months of age with 60% penetrance. The remarkably similar immunophenotypes and pathogenic transcriptional profiles of these lymphomas suggested that CBP loss acts to promote tumorigenesis in cooperation with a narrowly defined array of genetic changes. Further analyses indicated that downregulation of the tumor suppressor $p27^{Kip1}$ is a key determinant of CBP-mediated lymphomagenesis, and that key regulators of $p27^{Kip1}$ proteosomal degradation are overexpressed in CBP-null tumors.

Because p53-null mice develop fatal T cell lymphomas and because a multitude of studies have implicated CBP and p300 in the transactivation functions of p53 (Goodman and Smolik,

2000; Grossman, 2001), we initially hypothesized that CBP loss leads to tumor formation through inactivation of p53. However, five distinct lines of experimental evidence indicate that there is no loss of p53 tumor suppression activity in tumors that lack CBP. First, asymptomatic mutant mice with a substantial proportion of thymocytes lacking CBP protein exhibited no increased susceptibility to radiation-induced lymphomagenesis, implying that proper p53-mediated DNA repair and apoptosis occurred despite CBP deficiency. In fact, irradiated conditional knockout mice showed a somewhat reduced latency compared to their nonirradiated counterparts (see Figure 5A). The basis of this difference is unclear. One possible explanation is that it is caused by radiation-induced cell death, which normally occurs in thymocytes with an intact p53 response to DNA damage (Lowe et al., 1993). Since CBP-null tumors are clonally derived, the reduction in total thymocyte number in irradiated mice may outweigh the risk of radiation-induced tumors. Second, cells from tumors of moribund CBP conditional knockout mice responded to ionizing irradiation with p53 stabilization and induction of $p21^{Waf/Cip1}$, suggesting that the p53 response to DNA damage was intact (Figure 5B). Third, radiation-induced apoptosis was similar in cells from CBP-null tumors and thymocytes from control mice. Fourth, DNA microarray analysis revealed distinctive gene expression profiles for p53-null and CBP-null tumors, with at least 60 genes differentially expressed more than 2 fold, suggesting that the tumorigenic mechanisms operating in the two lymphoma types were distinct (Figure 5D). Fifth, double mutant mice lacking both CBP and p53 developed T cell lymphomas with significantly shorter latencies than mice with only CBP- or p53-null mutations (Figure 5C). This cooperative effect argues that the tumor suppression activities of CBP and p53 in T cell lymphomagenesis are not redundant. We note that although p53 loss can cooperate with CBP loss, lymphomagenesis in CBP conditional single knockout mice is unlikely to involve such cooperation, as both preleukemic and fully transformed thymocytes seem to have conserved p53 activity. The simplest explanation for finding that key p53 functions appear to be intact in CBP-null thymocytes would be that CBP and p300 are fully redundant for their functions in p53-dependent transcription and that p300 levels are sufficiently high to deliver these functions to p53. Alternatively, it is possible that CBP and p300 functions are distinct in thymocytes, with p300 exclusively providing adaptor molecule and protein acetyltransferase functions to p53. Testing for this possibility would require p300 conditional knockout mice, given the embryonic lethal phenotype associated complete p300 disruptions (Yao et al., 1998). There are also likely to be CBP-independent mechanisms important for p53 function.

Our findings suggest that $p27^{Kip1}$ insufficiency is a key cooperative event in CBP-mediated lymphomagenesis, and show that the mechanism of $p27^{Kip1}$ reduction in CBP tumors seems to involve decreased gene transcription and increased protein degradation. It seems unlikely that the observed reduction in $p27^{Kip1}$ mRNA levels is a direct consequence of CBP loss, because both $p27^{Kip1}$ mRNA and protein levels appeared normal in preleukemic thymocytes from CBP conditional knockout mice (Figures 6B, 6C, and 7D). However, one possibility is that the Myc oncoprotein, which is overexpressed in CBP-null tumors (Figures 7D and 8), and which has been reported to bind to and repress the $p27^{Kip1}$ gene promoter (Yang et al., 2001), causes the transcriptional reduction. We found that CBP-null tumors displayed several abnormalities that are consistent with increased $p27^{Kip1}$ protein degradation. Of these, the upregulation of Skp2, a key component of the SCF ubiquitin ligase complex that targets $p27^{Kip1}$ for destruction by the proteosome (Carrano et al., 1999), was perhaps the most prominent one. Skp2 has oncogenic properties (Latres et al., 2001), and is overexpressed in many human cancers, including lymphomas, where its level of expression seems to correlate with the grade of malignancy and inversely with $p27^{Kip1}$ levels (reviewed in Blain et al., 2003). A second abnormality was the upregulation of cyclin E. This cyclin normally accumulates in G_1 phase and targets $p27^{Kip1}$ protein for ubiquitin-mediated degradation by phosphorylation on tyrosine 187, and when expressed at high levels, it seems to increase $p27^{Kip1}$ phosphorylation and degradation (reviewed by Blain et al., 2003; Bloom and Pagano, 2003). CBP conditional knockout mice in which $p27^{Kip1}$ levels were lowered genetically by the introduction of a $p27^{Kip1}$-null allele produced tumors with relatively low Skp2 and cyclin E levels, a finding that supports the view that increases in Skp2 and cyclin E stimulate $p27^{Kip1}$ degradation during CBP-mediated lymphomagenesis (Figure 7B). Myc has also been implicated in ubiquitinated-mediated degradation of $p27^{Kip1}$ (Muller et al., 1997; O'Hagan et al., 2000). However, in CBP-null tumors, Myc overexpression may not be linked to $p27^{Kip1}$ degradation, because Myc levels remained highly increased in tumors from MMTV-Cre|$CBP^{flox/flox}$;$p27^{Kip1+/-}$ mice (Figure 7D). This interpretation is further supported by a study from Martins and Berns in which $p27^{Kip1}$ loss is shown to synergize with Myc overexpression in murine lymphomagenesis (Martins and Berns, 2002).

Two additional oncoproteins, Notch1 and Bmi-1, are expressed at very high levels in almost all CBP-null tumors. Given that overexpression of each of these proteins in mouse thymocytes has been shown to result in the development of T cell lymphomas (Alkema et al., 1997; Fowlkes and Robey, 2002; Haupt et al., 1993), it is tempting to speculate that they may play an active role in CBP-mediated lymphomagenesis. Because there was no detectable upregulation of Notch1 and Bmi-1 in thymocytes from preleukemic CBP conditional knockout mice, it seems that their role, if any, would be late rather than early in the transformation process. It will be of great interest to further investigate whether Notch1, Bmi-1 and Myc act synergistically with CBP loss by crossing CBP conditional knockout mice with transgenics overexpressing these genes.

In conclusion, our study illustrates that loss of the versatile transcriptional coactivator CBP leads to tumors with a distinctive pathogenic expression signature that includes several cancer-critical genes that are often deregulated in human lymphomas and associated with poor prognosis. Whether CBP is disrupted or functionally inactivated in human lymphomas remains to be investigated. The expression signature reported here might be a useful guide in the identification of cancers with CBP loss. In addition, the availability of CBP conditional knockout mice will provide a novel tool for further evaluation of the role of CBP in the development of cancer and for preclinical therapeutic studies.

Experimental procedures

Generation of CBP conditional knockout and compound mutant mice

CBP conditional knockout mice were generated as described in detail in the Supplemental Data at http://www.cancercell.org/cgi/content/full/5/2/177/

DC1. These mice were bred to MMTV-Cre transgenic mice (Wagner et al., 1997). Male MMTV-Cre|CBP$^{+/flox}$ mice were bred with CBP$^{flox/flox}$ females to produce MMTV-Cre|CBP$^{flox/flox}$ mice. MMTV-Cre|CBP$^{flox/flox}$;p53$^{-/-}$ and CBP$^{flox/flox}$;p53$^{-/-}$ animals were generated by breeding p53$^{-/-}$ mice to MMTV-Cre|CBP$^{flox/flox}$ mice. MMTV-Cre|CBP$^{flox/flox}$;p27$^{Kip1+/-}$ mice were produced by breeding p27$^{Kip1+/-}$ mice (Fero et al., 1996) to MMTV-Cre|CBP$^{flox/flox}$ mice. All mice used in the tumor-free survival studies described in this report were of a mixed 129 × C57BL/6 genetic background (to exclude effects of genetic background factors on tumor latency and penetrance). Mice were observed daily for signs of poor health. Sick mice were sacrificed and screened for tumors. Survival curves were prepared using GraphPad Prism software.

PCR genotyping of mice

CBP^{+}, CBP^{flox}, and CBP^{-} alleles were also genotyped by PCR. Primers used were CBP-F1 (5′-GGGGAAATTTTG GCTGGCAAG-3′) and CBP-R1 (5′-CTGCTCTACCTAAATTCCCAG-3′). These primers produce 1250, 1100, and 970 bp fragments for the CBP^{+}, CBP^{flox}, and CBP^{-} alleles, respectively. p53 and p27^{Kip1} were identified according to previously described PCR protocols (Fero et al., 1996; Jacks et al., 1994). The MMTV-Cre transgenic locus was identified as described (Wagner et al., 1997).

Tumor collection and histopathology

Moribund animals were sacrificed and major organs screened for overt tumors using a dissection microscope. Tumors were harvested and confirmed by standard histological analysis. Tumors were assayed for clonal TCR gene rearrangements by Southern analysis as previously described (Chervinsky et al., 1999).

Immunolabeling procedures

Cell suspensions from thymuses, lymph nodes, bone marrow, or T cell lymphomas were fixed with 3% paraformaldehyde in PBS for 15 min. Cells were then attached onto polyethylenimine-coated 12-well chambered microscope slides. Cells were permeabilized with 0.2% Triton-X-100/PBS for 5 min at RT and then blocked with 3% nonfat dry milk/PBS for 1 hr prior to primary antibody incubations. The following antibodies were used for staining: CBP(C-20) (sc-583, 1:800, Santa Cruz); p300(C-20) (sc-585, 1:800, Santa Cruz); CD8-FITC (1:50, BD Pharmingen); CD4-PE (1:50, BD Pharmingen); B220-FITC (1:100, BD Pharmingen); Gr-1-FITC (1:100, BD Pharmingen); p27^{Kip1} (K25020) (1:200, DB laboratories), and cyclin E (M-20) (1:200, sc-481, Santa Cruz). Secondary antibody incubations were as described (Kasper et al., 1999). Representative images were collected with a Zeiss confocal microscope (LSM510).

Western blot analysis

Western blot analysis was performed as described (Kasper et al., 1999). The following antibodies were used at 1:200 dilution (from Santa Cruz unless indicated otherwise): CBP(C20) (sc-583), CBP(A22) (sc-369), p53(FL-393)-G (sc-6243-G), p21$^{Waf1/Cip1}$(M-19) (sc-471), cyclin E(M-20) (sc-481), Bcl-X(L-19) (sc-1041), Bmi-1 (H99) (sc-10745), p27^{Kip1}(K25020) (Transduction Laboratory), p45^{Skp2} (SKP2-2B12, Zymed laboratories), Notch1 (mN1A, dilution 1: 200, BD Biosciences), and β-actin (AC-151, Sigma).

Immunophenotyping

Single-cell suspensions were prepared from thymus or tumor masses and stained antibodies (Pharmingen) were used: anti-CD8-FITC, anti-CD4-PE, anti-CD25-PE, anti-CD44-FITC, anti-CD3-FITC, and anti-TCRβ-FITC. Data were collected on 3 × 10^{4} events using a FACScan flow cytometer and analyzed using CellQuest software (Becton Dickinson). An unpaired Student's t test was used for statistical analysis.

Treatments with ionizing irradiation and MG132

MMTV-Cre|CBP$^{flox/flox}$ and CBP$^{flox/flox}$ littermates were exposed to 1 Gy whole body irradiation from a ^{137}Cs source at 14 and 21 days of age. For analysis of the p53 response to DNA damage, single-cell suspensions of thymus or tumor masses were freshly prepared as above and cultured in RPMI-1640 supplemented with 10% FCS, 0.055 mM β-mercaptoethanol, IL-2 (10 U/ml), PHA (5 μg/ml) and conA (5 μg/ml). The next day, they were exposed to 5 Gy γ irradiation. At 0, 4, and 8 hr post irradiation, cells were harvested and lysates were prepared. p53 and p21$^{Waf1/Cip1}$ protein levels were measured by Western blot analysis. For analysis of p27^{Kip1} proteolysis, cell suspensions were cultured in the presence of 25 μM MG132 (Boston Biochemical).

DNA microarray analysis

Thymus or tumor masses were collected from mice and homogenized for total RNA isolation with TRIzol reagent (Life Technologies). RNA samples were further processed for hybridization to AFFY_U74A or AFFY_MOE430A Genechips (Affymetrix, Santa Clara) by the Mayo Clinic Microarray and Molecular Epidemiology shared facility as previously described in detail (Stegall et al., 2002). The initial analysis was performed using Affymetrix Microarray Suite 5.0 with the default settings. The Data Mining Tool (DMT) program was used to further select genes that were present in all samples being compared and were differentially expressed by two or more fold (up- or downregulated). Probe sets scored as absent were excluded from the analysis. Signal values for the selected genes were clustered and heat maps generated using Cluster and TreeView 1.6 software.

Quantitative RT-PCR

cDNA was generated from 200 ng of total RNA using SuperScript II RNase H^{-} reverse transcriptase and 9-mer random primers. Primer sequences and details of the real-time RT-PCR analysis are described in the Supplemental Experimental Procedures at http://www.cancercell.org/cgi/content/full/5/2/177/DC1.

Acknowledgments

We thank Peter Aplan for the TCR Cβ2 probe. We thank Rick Bram, Fergus Couch, David McKean, Junjie Chen, Larry Karnitz, Janine van Ree, and Ralf Janknecht for critically reviewing our manuscript, helpful discussions, or reagents. We are grateful to Karthik Jeganathan for help with various Western blot analyses. This work was supported by DOD IDEA AWARD BC010517, NIH grants R01-CA76385 and P30-CA21765, and the American Lebanese Syrian Associated Charities of St. Jude Children's Research Hospital.

Received: June 30, 2003
Revised: December 23, 2003
Accepted: January 6, 2003
Published: February 23, 2004

References

Alkema, M.J., Bronk, M., Verhoeven, E., Otte, A., van't Veer, L.J., Berns, A., and van Lohuizen, M. (1997). Identification of Bmi1-interacting proteins as constituents of a multimeric mammalian polycomb complex. Genes Dev. *11*, 226–240.

Avantaggiati, M.L., Ogryzko, V., Gardner, K., Giordano, A., Levine, A.S., and Kelly, K. (1997). Recruitment of p300/CBP in p53-dependent signal pathways. Cell *89*, 1175–1184.

Blain, S.W., Scher, H.I., Cordon-Cardo, C., and Koff, A. (2003). p27 as a target for cancer therapeutics. Cancer Cell *3*, 111–115.

Blobel, G.A. (2000). CREB-binding protein and p300: Molecular integrators of hematopoietic transcription. Blood *95*, 745–755.

Bloom, J., and Pagano, M. (2003). Deregulated degradation of the cdk inhibitor p27 and malignant transformation. Semin. Cancer Biol. *13*, 41–47.

Carrano, A.C., Eytan, E., Hershko, A., and Pagano, M. (1999). SKP2 is required for ubiquitin-mediated degradation of the CDK inhibitor p27. Nat. Cell Biol. *1*, 193–199.

Catzavelos, C., Bhattacharya, N., Ung, Y.C., Wilson, J.A., Roncari, L., Sandhu, C., Shaw, P., Yeger, H., Morava-Protzner, I., Kapusta, L., et al. (1997). Decreased levels of the cell-cycle inhibitor p27Kip1 protein: prognostic implications in primary breast cancer. Nat. Med. *3*, 227–230.

Chervinsky, D.S., Zhao, X.F., Lam, D.H., Ellsworth, M., Gross, K.W., and Aplan, P.D. (1999). Disordered T-cell development and T-cell malignancies in SCL LMO1 double-transgenic mice: parallels with E2A-deficient mice. Mol. Cell. Biol. *19*, 5025–5035.

Deguchi, K., Ayton, P.M., Carapeti, M., Kutok, J.L., Snyder, C.S., Williams, I.R., Cross, N.C., Glass, C.K., Cleary, M.L., and Gilliland, D.G. (2003). MOZ-TIF2-induced acute myeloid leukemia requires the MOZ nucleosome binding motif and TIF2-mediated recruitment of CBP. Cancer Cell *3*, 259–271.

Erlanson, M., Portin, C., Linderholm, B., Lindh, J., Roos, G., and Landberg, G. (1998). Expression of cyclin E and the cyclin-dependent kinase inhibitor p27 in malignant lymphomas-prognostic implications. Blood *92*, 770–777.

Fero, M.L., Rivkin, M., Tasch, M., Porter, P., Carow, C.E., Firpo, E., Polyak, K., Tsai, L.H., Broudy, V., Perlmutter, R.M., et al. (1996). A syndrome of multiorgan hyperplasia with features of gigantism, tumorigenesis, and female sterility in p27(Kip1)-deficient mice. Cell *85*, 733–744.

Fero, M.L., Randel, E., Gurley, K.E., Roberts, J.M., and Kemp, C.J. (1998). The murine gene p27Kip1 is haplo-insufficient for tumour suppression. Nature *396*, 177–180.

Fowlkes, B.J., and Robey, E.A. (2002). A reassessment of the effect of activated Notch1 on CD4 and CD8 T cell development. J. Immunol. *169*, 1817–1821.

Gayther, S.A., Batley, S.J., Linger, L., Bannister, A., Thorpe, K., Chin, S.F., Daigo, Y., Russell, P., Wilson, A., Sowter, H.M., et al. (2000). Mutations truncating the EP300 acetylase in human cancers. Nat. Genet. *24*, 300–303.

Giordano, A., and Avantaggiati, M.L. (1999). p300 and CBP: Partners for life and death. J. Cell. Physiol. *181*, 218–230.

Goodman, R.H., and Smolik, S. (2000). CBP/p300 in cell growth, transformation, and development. Genes Dev. *14*, 1553–1577.

Grossman, S.R. (2001). p300/CBP/p53 interaction and regulation of the p53 response. Eur. J. Biochem. *268*, 2773–2778.

Gu, W., Shi, X.L., and Roeder, R.G. (1997). Synergistic activation of transcription by CBP and p53. Nature *387*, 819–823.

Haupt, Y., Bath, M.L., Harris, A.W., and Adams, J.M. (1993). bmi-1 transgene induces lymphomas and collaborates with myc in tumorigenesis. Oncogene *8*, 3161–3164.

Ito, A., Lai, C.H., Zhao, X., Saito, S., Hamilton, M.H., Appella, E., and Yao, T.P. (2001). p300/CBP-mediated p53 acetylation is commonly induced by p53-activating agents and inhibited by MDM2. EMBO J. *20*, 1331–1340.

Jacks, T., Remington, L., Williams, B.O., Schmitt, E.M., Halachmi, S., Bronson, R.T., and Weinberg, R.A. (1994). Tumor spectrum analysis in p53-mutant mice. Curr. Biol. *4*, 1–7.

Jacobs, J.J., Scheijen, B., Voncken, J.W., Kieboom, K., Berns, A., and van Lohuizen, M. (1999). Bmi-1 collaborates with c-Myc in tumorigenesis by inhibiting c-Myc-induced apoptosis via INK4a/ARF. Genes Dev. *13*, 2678–2690.

Kasper, L.H., Brindle, P.K., Schnabel, C.A., Pritchard, C.E., Cleary, M.L., and van Deursen, J.M. (1999). CREB binding protein interacts with nucleoporin-specific FG repeats that activate transcription and mediate NUP98-HOXA9 oncogenicity. Mol. Cell. Biol. *19*, 764–776.

Kasper, L.H., Boussouar, F., Ney, P.A., Jackson, C.W., Rehg, J., van Deursen, J.M., and Brindle, P.K. (2002). A transcription-factor-binding surface of coactivator p300 is required for haematopoiesis. Nature *419*, 738–743.

Kee, B.L., Arias, J., and Montminy, M.R. (1996). Adaptor-mediated recruitment of RNA polymerase II to a signal-dependent activator. J. Biol. Chem. *271*, 2373–2375.

Kemp, C.J., Wheldon, T., and Balmain, A. (1994). p53-deficient mice are extremely susceptible to radiation-induced tumorigenesis. Nat. Genet. *8*, 66–69.

Kung, A.L., Rebel, V.I., Bronson, R.T., Ch'ng, L.E., Sieff, C.A., Livingston, D.M., and Yao, T.P. (2000). Gene dose-dependent control of hematopoiesis and hematologic tumor suppression by CBP. Genes Dev. *14*, 272–277.

Latres, E., Chiarle, R., Schulman, B.A., Pavletich, N.P., Pellicer, A., Inghirami, G., and Pagano, M. (2001). Role of the F-box protein Skp2 in lymphomagenesis. Proc. Natl. Acad. Sci. USA *98*, 2515–2520.

Li, M., Luo, J., Brooks, C.L., and Gu, W. (2002). Acetylation of p53 inhibits its ubiquitination by Mdm2. J. Biol. Chem. *277*, 50607–50611.

Lill, N.L., Grossman, S.R., Ginsberg, D., DeCaprio, J., and Livingston, D.M. (1997). Binding and modulation of p53 by p300/CBP coactivators. Nature *387*, 823–827.

Liu, L., Scolnick, D.M., Trievel, R.C., Zhang, H.B., Marmorstein, R., Halazonetis, T.D., and Berger, S.L. (1999). p53 sites acetylated in vitro by PCAF and p300 are acetylated in vivo in response to DNA damage. Mol. Cell. Biol. *19*, 1202–1209.

Loda, M., Cukor, B., Tam, S.W., Lavin, P., Fiorentino, M., Draetta, G.F., Jessup, J.M., and Pagano, M. (1997). Increased proteasome-dependent degradation of the cyclin-dependent kinase inhibitor p27 in aggressive colorectal carcinomas. Nat. Med. *3*, 231–234.

Lowe, S.W., Schmitt, E.M., Smith, S.W., Osborne, B.A., and Jacks, T. (1993). p53 is required for radiation-induced apoptosis in mouse thymocytes. Nature *362*, 847–849.

Lu, Q., Hutchins, A.E., Doyle, C.M., Lundblad, J.R., and Kwok, R.P. (2003). Acetylation of cAMP-responsive element-binding protein (CREB) by CREB-binding protein enhances CREB-dependent transcription. J. Biol. Chem. Published online February 20, 2003. 10.1074/jbc.M300546200.

Martins, C.P., and Berns, A. (2002). Loss of p27(Kip1) but not p21(Cip1) decreases survival and synergizes with MYC in murine lymphomagenesis. EMBO J. *21*, 3739–3748.

Muhua, L., Adames, N.R., Murphy, M.D., Shields, C.R., and Cooper, J.A. (1998). A cytokinesis checkpoint requiring the yeast homologue of an APC-binding protein. Nature *393*, 487–491.

Muller, D., Bouchard, C., Rudolph, B., Steiner, P., Stuckmann, I., Saffrich, R., Ansorge, W., Huttner, W., and Eilers, M. (1997). Cdk2-dependent phosphorylation of p27 facilitates its Myc-induced release from cyclin E/cdk2 complexes. Oncogene *15*, 2561–2576.

Nakajima, T., Uchida, C., Anderson, S.F., Lee, C.G., Hurwitz, J., Parvin, J.D., and Montminy, M. (1997). RNA helicase A mediates association of CBP with RNA polymerase II. Cell *90*, 1107–1112.

O'Hagan, R.C., Ohh, M., David, G., de Alboran, I.M., Alt, F.W., Kaelin, W.G., Jr., and DePinho, R.A. (2000). Myc-enhanced expression of Cul1 promotes ubiquitin-dependent proteolysis and cell cycle progression. Genes Dev. *14*, 2185–2191.

Ogryzko, V.V., Schiltz, R.L., Russanova, V., Howard, B.H., and Nakatani, Y. (1996). The transcriptional coactivators p300 and CBP are histone acetyltransferases. Cell *87*, 953–959.

Oike, Y., Takakura, N., Hata, A., Kaname, T., Akizuki, M., Yamaguchi, Y., Yasue, H., Araki, K., Yamamura, K., and Suda, T. (1999). Mice homozygous for a truncated form of CREB-binding protein exhibit defects in hematopoiesis and vasculo-angiogenesis. Blood *93*, 2771–2779.

Ozdag, H., Batley, S.J., Forsti, A., Iyer, N.G., Daigo, Y., Boutell, J., Arends, M.J., Ponder, B.A., Kouzarides, T., and Caldas, C. (2002). Mutation analysis of CBP and PCAF reveals rare inactivating mutations in cancer cell lines but not in primary tumours. Br. J. Cancer *87*, 1162–1165.

Petrij, F., Giles, R.H., Dauwerse, H.G., Saris, J.J., Hennekam, R.C., Masuno, M., Tommerup, N., van Ommen, G.J., Goodman, R.H., Peters, D.J., et al. (1995). Rubinstein-Taybi syndrome caused by mutations in the transcriptional co-activator CBP. Nature *376*, 348–351.

Porter, P.L., Malone, K.E., Heagerty, P.J., Alexander, G.M., Gatti, L.A., Firpo, E.J., Daling, J.R., and Roberts, J.M. (1997). Expression of cell-cycle regulators p27Kip1 and cyclin E, alone and in combination, correlate with survival in young breast cancer patients. Nat. Med. *3*, 222–225.

Rebel, V.I., Kung, A.L., Tanner, E.A., Yang, H., Bronson, R.T., and Livingston, D.M. (2002). Distinct roles for CREB-binding protein and p300 in hematopoietic stem cell self-renewal. Proc. Natl. Acad. Sci. USA *99*, 14789–14794.

Sakaguchi, K., Herrera, J.E., Saito, S., Miki, T., Bustin, M., Vassilev, A., Anderson, C.W., and Appella, E. (1998). DNA damage activates p53 through a phosphorylation-acetylation cascade. Genes Dev. *12*, 2831–2841.

Stegall, M., Park, W., Kim, D., and Kremers, W. (2002). Gene expression during acute allograft rejection: Novel statistical analysis of microarray data. Am. J. Transplant. *2*, 913–925.

Wagner, K.U., Wall, R.J., St-Onge, L., Gruss, P., Wynshaw-Boris, A., Garrett, L., Li, M., Furth, P.A., and Hennighausen, L. (1997). Cre-mediated gene deletion in the mammary gland. Nucleic Acids Res. *25*, 4323–4330.

Yang, W., Shen, J., Wu, M., Arsura, M., FitzGerald, M., Suldan, Z., Kim, D.W., Hofmann, C.S., Pianetti, S., Romieu-Mourez, R., et al. (2001). Repression of transcription of the p27(Kip1) cyclin-dependent kinase inhibitor gene by c-Myc. Oncogene *20*, 1688–1702.

Yao, T.P., Oh, S.P., Fuchs, M., Zhou, N.D., Ch'ng, L.E., Newsome, D., Bronson, R.T., Li, E., Livingston, D.M., and Eckner, R. (1998). Gene dosage-dependent embryonic development and proliferation defects in mice lacking the transcriptional integrator p300. Cell *93*, 361–372.